JOURNAL OF APPLIED ELECTROCHEMISTRY 25 (1995) 106–113

Comparison of the behaviour of glassy carbon and some metals for use as nonconsumable anodes in alumina–cryolite melts

S. S. DJOKIĆ,* B. E. CONWAY

Department of Chemistry, University of Ottawa, Ottawa, Ontario, Canada K1N 6N5

Received 3 February 1994; revised 3 June 1994

Current interest exists in development of nonconsumable anodes for the Hall–Héroult process of aluminium production and also *in situ* analytical probes for determination of Al_2O_3 content in the cryolite melts used in this process. A comparison of the behaviour of glassy carbon and metals such as tungsten, tungsten carbide, nickel and stainless steel (SS-316) used as anodes in alumina–cryolite melts is investigated by means of electrochemical transient techniques (cyclic voltammetry and chronoamperometry) and Tafel anodic polarization experiments. The results show that only glassy carbon could be used as a successful sensor electrode for an *in situ* determination of Al_2O_3 in alumina–cryolite melts and that the metals investigated are unresistant to anodic attack in such melts. Consequently, the metals investigated cannot be used as sensor electrodes for *in situ* electroanalytical determination of alumina in alumina–cryolite melts, nor as anodes in the production of aluminium by the Hall–Héroult process.

1. Introduction

The principal basis for production of aluminium metal by the Hall–Héroult process with a consumable graphite anode can simply be described in terms of the following reactions, for which the respective, thermodynamically calculated E^0 values are indicated as shown:

$$Al_2O_3 + \tfrac{3}{2}C \rightleftharpoons 2Al + \tfrac{3}{2}CO_2 \quad (E^0 = 1.163\,V \text{ at } 1010^\circ C) \tag{1}$$

and

$$Al_2O_3 + 3C \rightleftharpoons 2Al + 3CO \quad (E^0 = 1.024\,V \text{ at } 1010^\circ C) \tag{2}$$

Consumable carbon anodes have long been used and have become of major significance in the technology of aluminium production practice. However, recently, the possibility of using inert, or so-called 'nonconsumable', anodes has become attractive for the following reasons:

(i) Inert anodes would not be consumed during electrolysis.

(ii) The oxygen which would then be formed at the anode could be utilized industrially.

(iii) The problems related to contamination of the working environment, when the Hall–Héroult process is used could be reduced.

(iv) The corresponding cell design would permit electrolysis with higher current efficiencies than is currently possible with carbon anodes.

(v) All the above mentioned factors could represent significant savings to the aluminium production industry.

In the case of inert (nonconsumable) anodes, the production of aluminium would be represented formally by the equation:

$$Al_2O_3 \rightleftharpoons \tfrac{3}{2}O_2 + 2Al \quad (E^0 = -2.19\,V \text{ at } 1010^\circ C) \tag{3}$$

In the search for an inert anode for use in Hall–Héroult electrolysis, among many accessible materials, oxides, metals, refractory hard metals and gaseous-fuel anodes have been investigated. Among the oxides, investigated as materials for anodes in electrolysis of an alumina–cryolite melt should be mentioned the cold pressed and sintered anodes of Fe_3O_4, SnO_2, Co_2O_4, NiO, CuO and Cr_2O_3 [1], the ferrites such as $SnO_2 \cdot Fe_2O_3$, $NiO \cdot Fe_2O_3$ and $ZnO \cdot Fe_2O_3$ [2], stabilized ZrO_2 as a possible inert material for production of less corrosion resistant anodes [3], the SnO_2-based anodes [4–6] and complex oxides with a base of Y_2O_3 [7]. The Cu-containing cermets ($NiFe_2O_4$ spinel, NiO and a metallic phase which was mostly Cu) have also been investigated as possible anode materials for the primary aluminium industry [8].

In the case of gaseous-fuel anodes, the production of aluminium metal can be described [9] by the following reactions:

$$Al_2O_3 + \tfrac{3}{4}CH_4 \rightleftharpoons 2Al + \tfrac{3}{2}H_2O \tag{4}$$

$$Al_2O_3 + 3H_2 \rightleftharpoons 2Al + 3H_2O \tag{5}$$

* Present address: Sherritt Inc., Fort Saskatchewan, Alberta T8L 3W4, Canada.

0021-891X

Several authors have investigated this type of anode process for aluminium production [10–12].

The hard refractory materials such as borides, carbides and nitrides of the transition metals have also been tested as inert anode materials, among which should be mentioned the following: TiB_2 and TiB_2–BN mixtures [13], TiC, ZrB_2, MoSi and TiCr [14].

Various metal anodes for application in alumina–cryolite melts have also been investigated. Metals such as copper, nickel, chromium and silver, according to Belyaev and Studentsov's results [1, 8, 13] are unresistant. Experiments with platinum [15–17] and gold [17], as anodes in alumina–cryolite melts, showed formation of an oxide film on the electrode surface and/or corrosion. Platinum anode corrosion occurred at high current densities [15] in a melt without Al_2O_3 as well as in melts saturated with Al_2O_3. Such behaviour was attributed to discharge of F^-. Metallic anodes are usually not completely inert, because of their tendency to become oxidized. Although, in general, such processes usually depend on the physical and chemical properties of the metal, reactions involving the anode material and alumina can be represented by the following equation:

$$Al_2O_3(\text{cryolite}) + nM(s) \rightleftharpoons M_nO_3 + 2Al(l) \quad (6)$$

In the present work the behaviour of materials such as glassy carbon, W, Ni, stainless steel (SS-316) and WC has been examined comparatively by means of various transient or nonsteady-state electroanalytical techniques, not so much for the possibility of their use as the main anodes for industrial electrolytic production of aluminium, as for their applicability as anode probes for *in situ* electroanalytical determination of Al_2O_3 in the cryolite electrolyte [18, 19]. For such a purpose, either a nonreactive, i.e. nonconsumable, anode is also required so that either a direct electroanalytical response current, proportional to the Al_2O_3 content of the melt associated with oxygen evolution, is produced, or a very reactive consumable anode is required so that its oxidation rate is limited by diffusion of the O-containing ions in the melt, arising from the Al_2O_3 to be determined.

2. Experimental details

In the present work, the study of the anodic processes at glassy carbon and several metal anodes in cryolite/alumina melts has involved investigation of the type of anode material by means of comparative examination of their behaviour using electrochemical measurement techniques such as cyclic voltammetry and chronoamperometry, as well as by their anodic Tafel polarization responses.

Experiments were carried out in an open graphite crucible exposed to the atmosphere in a manner similar to that involved in industrial practice and also as outlined in previous papers [18, 19]. A bath containing 650 g Na_3AlF_6 (product of Bayer), 30 g Baker reagent-grade CaF_2, 22 g Al metal (to simulate conditions similar to those in industrial cells) with additions of Al_2O_3 (reagent grade) was used for investigations of the anodic reactions. The anodes consisted of rods of metals such as W, WC, Ni and SS-316 or glassy carbon sealed inside cylindrical boron nitride holders. The exposed surface areas of the working electrodes were 2.5 mm^2, 4.5 mm^2, 1 mm^2, 2.4 mm^2 and 7.5 mm^2 for W, WC, Ni, SS-316 and glassy carbon, respectively. The counter electrode (a graphite rod having a diameter of 1 cm) was immersed to a depth of about 2 cm into the melt. An aluminium metal reference electrode was housed in a separate boron nitride compartment provided with a small hole giving access to the melt. The experiments were carried out at $\sim$ 1010° C in a thermostatically controlled electric furnace.

The electrochemical measurements were carried out using a universal potentiostat/galvanostat (PAR model 273). Prior to performing experiments, as well as after experimentation, the surfaces of the working electrodes were examined by means of scanning electron microscopy (SEM).

3. Results and discussion

3.1. *Tungsten electrode*

The open-circuit potential at this metal was not stable

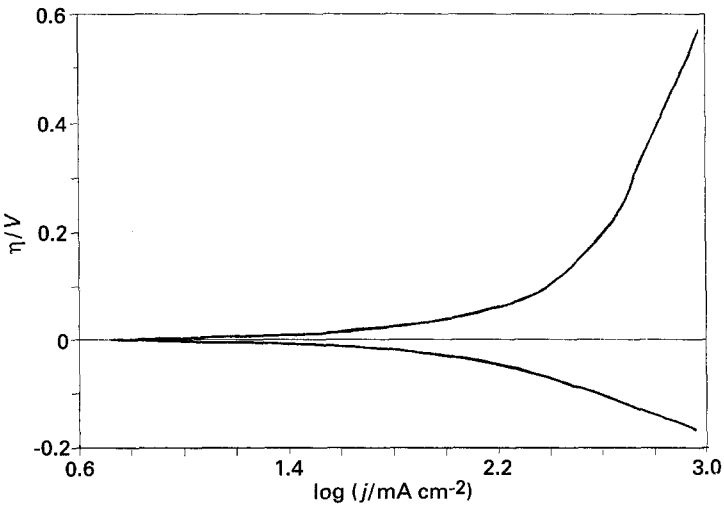

Fig. 1. Anodic Tafel polarization curve for tungsten electrode in cryolite melt at 1010° C with 20 g of added Al_2O_3.

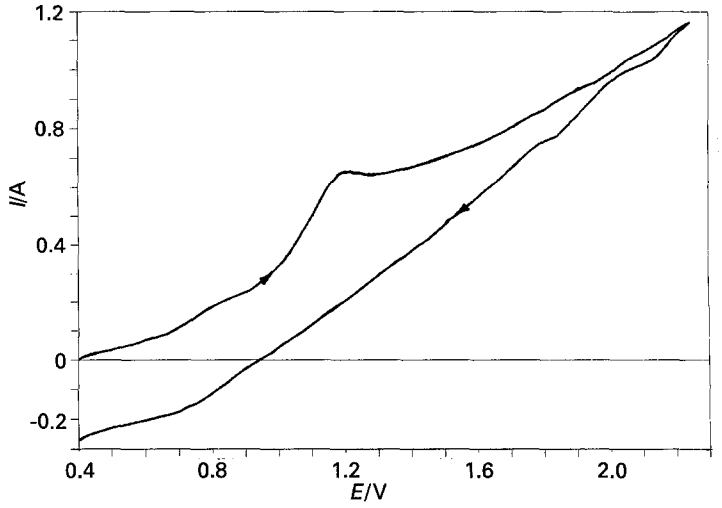

Fig. 2. Cyclic voltammogram obtained at the tungsten working electrode (sweep rate 60 V s^{-1}, 20 g Al_2O_3 present in the melt).

and had values between 0.06–0.17 V with respect to the aluminium reference electrode. A typical anodic Tafel plot is shown in Fig. 1. It is clear that the anodic processes involved are not under diffusion control. Thus, the quantity of alumina in the electrolyte did not systematically affect the values of exchange current density. In other words, the plot of exchange current density (determined by extrapolation of the Tafel relations) or of current densities at higher potentials vs Al_2O_3 concentration did not give a smooth relationship.

Figure 2 shows a cyclic voltammogram obtained at a tungsten working electrode over the potential range 0.4 to 2.25 V vs Al. In the region of increasing current, two anodic peaks can be seen: the first at about 0.83 V and the second at about 1.2 V. In the negative-going sweep direction, a cathodic current peak at about 0.8 V is observed (Fig. 2).

It was found that, with increase of square-root of sweep rate, the anodic peak current at about 1.2 V increases. However, this dependence does not follow a smooth linear relationship typical of a diffusion-controlled process. This behaviour corresponds to the shapes of the Tafel plots obtained for the tungsten electrode. The dependencies of peak currents on Al_2O_3 concentration do not follow any significant systematic trend suitable as a basis for an analytical application.

The chronoamperometric experiments were restricted to responses to potential steps from the open-circuit potential to 1.2 V. The potential of 1.2 V was chosen because the peak at that potential was the most reproducible one. The plot of I^{-1} vs $t^{1/2}$, in the chronoamperometric experiments, again did not follow a linear relationship typical of a diffusion controlled process, which is consistent with the cyclic voltammetry measurements, as well as with the shapes of the Tafel plots for the tungsten electrode.

Under the investigated conditions, it seems that only three anodic processes should be possible: (i) discharge of O^{2-} or other oxygen-containing species, (ii) discharge of F^- and (iii) dissolution of W or oxide film formation at the W surface.

Taking into consideration that the experiments were restricted to a maximum potential of 2.4 V and in analogy to similar processes on graphite anodes, it can be concluded that the discharge of F^- (or some corresponding complex-ion species) takes place only at more positive potentials [16]. The dissolution of tungsten is probably a chemical process under the investigated conditions, arising from anodic formation of WO_3. It has been reported [16] that 87.2% of WO_3 can be dissolved in cryolite media at elevated temperatures.

The anodic oxidation at tungsten electrodes may first of all be related to discharge of oxygen-containing species. The discharge of such species at a tungsten electrode is under mixed control. If oxygen species were being discharged as gaseous oxygen, substantial amounts of gas should be visible. Under these conditions, the tungsten would react with the oxygen according to the following reaction:

$$O_2 + W = WO_2 \qquad (7)$$

having an $E^0 = 0.73$ V at 1010° C (calculated from thermodynamic data), which corresponds reasonably to the observed potential of the anodic peak at about 0.8 V.

It is possible to correlate the peak at about 1.2 V with the following reaction:

$$3WO_2 + 4Al \rightleftharpoons 2Al_2O_3 + 3W \qquad (8)$$

which has $E^0 = 1.14$ V at 1010° C.

Under the conditions investigated, the following reactions are also possible:

$$2WO_2 + O_2 \rightleftharpoons 2WO_3 \qquad (9)$$

and

$$W + 3O_2 \rightleftharpoons 2WO_3 \qquad (10)$$

The tungsten oxides are acidic and could react chemically with bases. Thus, the tungsten electrode may be consumed in cryolite melts, which is clearly confirmed by photos from SEM examination and from literature data on dissolution of WO_3 in cryolite melts [16]. The cathodic peak may be related to the reverse of the reaction in Equation 8.

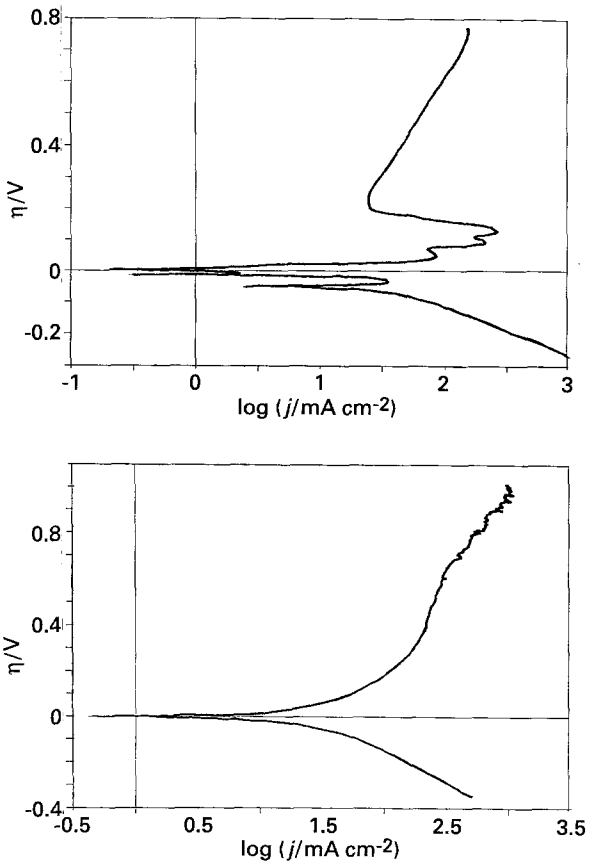

Fig. 3. Anodic Tafel polarization curve for a tungsten carbide working electrode (a) 0 g Al_2O_3, (b) 20 g Al_2O_3 added to the cryolite melt.

3.2. *Tungsten carbide electrode*

The results at a tungsten carbide electrode showed a high degree of nonreproducibility. The open-circuit potential had values between 0.2 V and 0.5 V.

The anodic Tafel plots, based on experiments at a tungsten carbide electrode in the cryolite melt without addition of alumina, show that passivation of the working electrode sets in. This is clearly illustrated in Fig. 3(a). It is noted that similar behaviour arose when 5 g of alumina were added to the melt. However, after 5 h delay, the passivation current becomes minimized. With further addition of alumina, the passivation current was not observed. A typical example is presented in Fig. 3(b).

In the first cycle of cyclic voltammetry experiments, unexpectedly high anodic currents arise. This behaviour is observed at the beginning and for experiments where no alumina had been added to the melt. However, for voltammograms recorded on succeeding cycles, the above mentioned behaviour was not observed. To avoid this background current, experiments were restricted to small sweep rates, less than $1\,V\,s^{-1}$. In the resulting cyclic voltammograms an anodic current peak arises at about 1.3 V (Fig. 4). Unfortunately, no meaningful dependence of this peak current on sweep rate and/or alumina concentration was found. Figure 4 shows indications (ripples, but no cathodic wave) for potentials above about 1.8 V. This could be attributed to the oxygen evolution reaction, forming, with tungsten carbide, WO_2 and/or WO_3, which become dissolved in the cryolite melt at elevated temperatures (see discussion below).

The results obtained by means of the chronoamperometric technique are impaired by noise which was shown not to be simply instrumental in origin. According to the chronoamperometric experiments, as for cyclic voltammetry, any significant dependence of the corresponding current functions, evaluated from the chronoamperograms, on alumina concentration, is not observable.

SEM photographs showed that, at the tungsten carbide electrode, material consumption had also been occurring. It was found, however, that in the case of this material, the surface has been changed *much less* than in the case of experiments with pure tungsten or other anode materials.

Because of the oxygen evolution reaction, the passivation of tungsten carbide is probably related to, or originates from, the reaction:

$$WC + 2O_2 \rightleftharpoons WO_2 + CO_2 \qquad (11)$$

It is obvious that substantial amounts of oxygen would be consumed in Reaction 11 by formation of CO_2 from the carbon component of WC as well as by formation of WO_2. In the following step, when

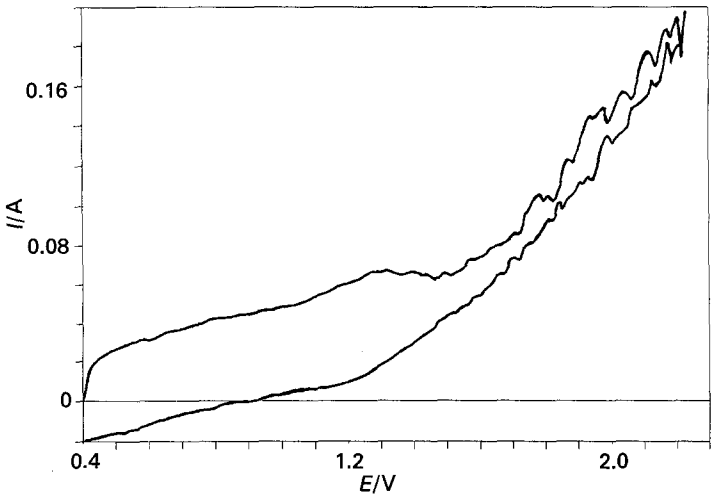

Fig. 4. Cyclic voltammogram for the tungsten carbide working electrode (5 g Al_2O_3, sweep rate $0.5\,V\,s^{-1}$).

the carbon is not available for the reaction with oxygen, which occurs in the melt at the WC after a delay, and/or with addition of Al_2O_3, oxygen will react with WO_2 according to the process:

$$2WO_2 + O_2 \rightleftharpoons 2WO_3 \qquad (12)$$

As mentioned, WO_3 oxide could be dissolved in cryolite melts, leading, in this way, to consumption of the WC electrode with resulting visible morphological changes.

3.3. *Nickel electrode*

The open-circuit potential of this anode had values 0.2–0.3 V. Anodic Tafel polarization curves for the nickel electrode are shown in Fig. 5. It seems, according to the shapes of the polarization curves, that addition of alumina to the cryolite melt leads to passivation (compare results in Fig. 5(a) and (b)).

Similarly, the chronoamperometric results do not show any smooth linear relationship between I^{-1} and $t^{1/2}$ as expected for diffusion control. In addition, these experiments again showed a high degree of nonreproducibility.

The application of fast cyclic voltammetry, was also not successful for sweep rates higher than 20 V s^{-1} for melts saturated with alumina and for sweep rates greater than 40 V s^{-1} for melts with low alumina content. In most cases, fast cyclic voltammetry measurements did not show any usefully distinguishable cathodic and/or anodic peaks. One example is

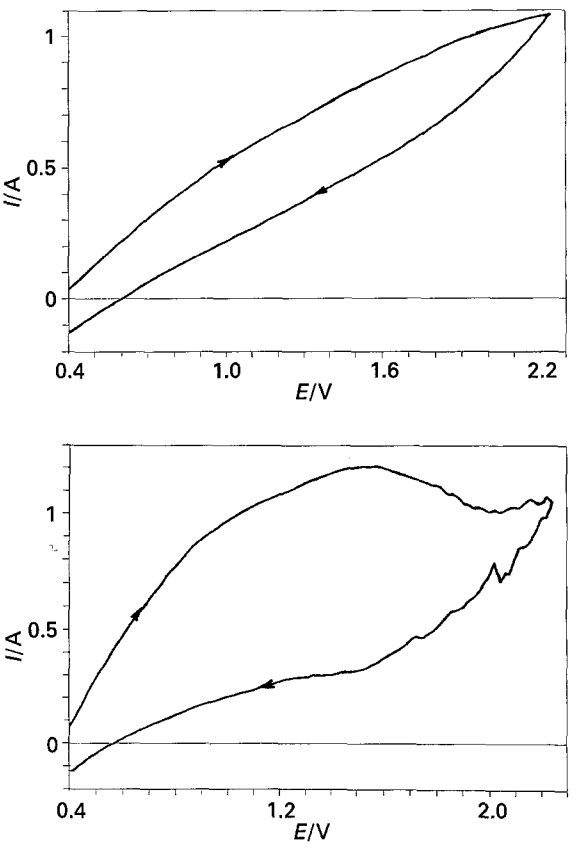

Fig. 6. Cyclic voltammogram for the nickel working electrode (a) 10 g Al_2O_3, sweep rate 20 V s^{-1}; (b) 5 g Al_2O_3, sweep rate 10 V s^{-1}.

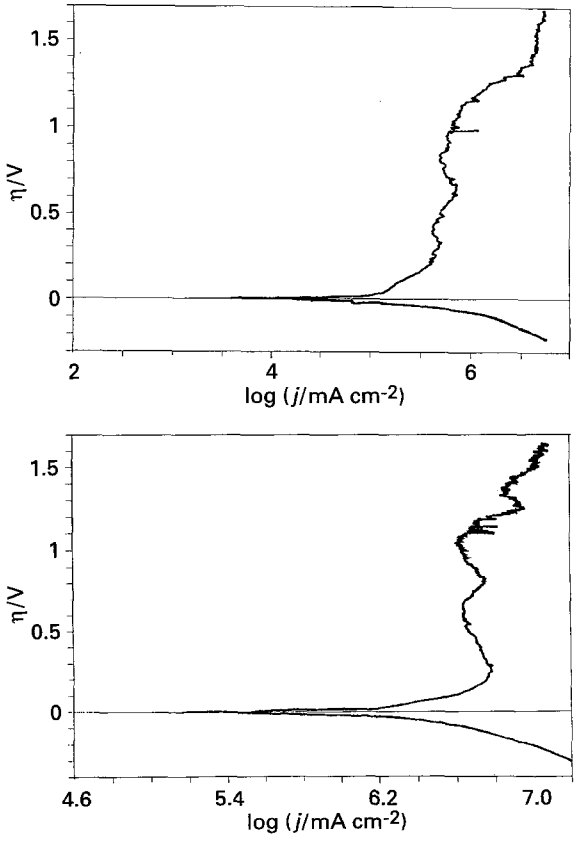

Fig. 5. Anodic Tafel polarization curve for a nickel working electrode (a) 0 g Al_2O_3, (b) 20 g Al_2O_3 added in the cryolite melt.

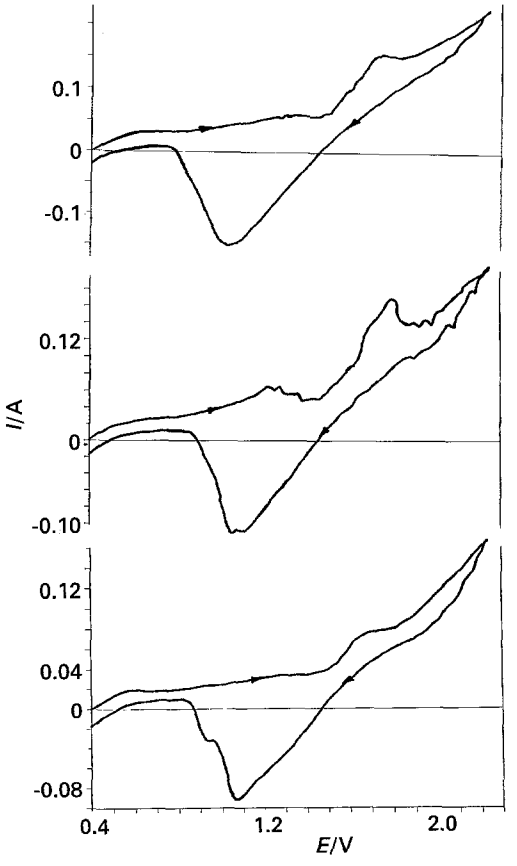

Fig. 7. Cyclic voltammogram for the nickel working electrode (a) 5 g Al_2O_3 present, sweep rate 0.1 V s^{-1}; (b) 10 g Al_2O_3, sweep rate 0.1 V s^{-1}; (c) 20 g Al_2O_3, sweep rate 0.1 V s^{-1}.

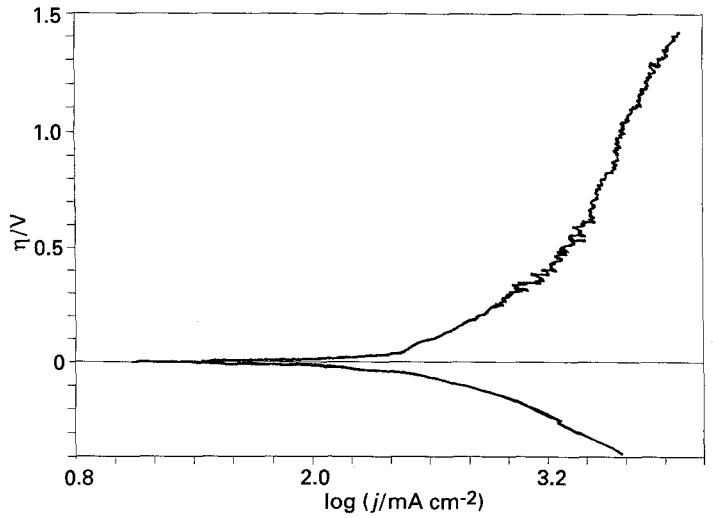

Fig. 8. Anodic Tafel polarization curve for a stainless steel working electrode (40 g Al_2O_3 added in the cryolite melt).

presented in Fig. 6(a). However, in the case of lower concentrations of Al_2O_3, as seen in Fig. 6(b), an anodic peak at about 1.5 V is observable.

More interesting behaviour was found when cyclic voltammetry at sweep rates less than $10\,V\,s^{-1}$ was applied; several examples are shown in Fig. 7, where two current peaks or current response waves are distinguishable: an anodic one at about 1.7 V and a cathodic one at about 1.0 V. Similar shapes of voltammograms were recently reported by Windisch and Marshman [8] for the case of Cu and Cu-containing cermet anodes in alumina–cryolite melts. The oxidation peak at about 2.16–2.20 V at 970° C was explained in terms of the following reaction:

$$Cu_2O(s) + Al_2O_3 \rightleftharpoons 2CuO(s) + O_2(g) + 2Al \quad (13)$$

The reduction peak at 2.00 V was assigned to the reverse of Reaction 13.

In analogy with their explanation, the oxidation peak in the present work at about 1.6 V could be associated with the reaction

$$3NiO + 2Al \rightleftharpoons 3Ni + Al_2O_3 \quad (14)$$

which has a standard potential at 1010° C of 1.61 V (value calculated from thermodynamic data). One possible source of the NiO is that it is formed chemically by reaction of Ni with Al_2O_3 in the molten cryolite prior to recording the cyclic voltammograms. Another possibility is that the oxide was part of an original air-formed film. However, the most likely source of NiO is anodic oxidation according to Equation 14. The cathodic peak at about 1.0 V could then be attributed to the reverse of Reaction 14.

It was found by SEM photography that the nickel anode, like tungsten, had also been consumed.

3.4. *Stainless steel electrode*

The open-circuit potential at this electrode gradually changed with time and also shifted with increase of alumina concentration in the melt. It had a value of about 0.26 V at the beginning, when alumina was not added, and about 0.45 V later, when the melt contained 40 g of Al_2O_3.

The anodic Tafel polarization plots shown in Fig. 8 exhibit two straight segments as also found at tungsten. Similar results were obtained with higher Al_2O_3 concentrations.

Figure 9 shows the cyclic voltammogram obtained at the stainless steel electrode. The application of fast cyclic voltammetry, as in the case of the nickel working electrode, was not successful for sweep rates higher than $10\,V\,s^{-1}$ in the case of the melt not containing any alumina. Consequently, these

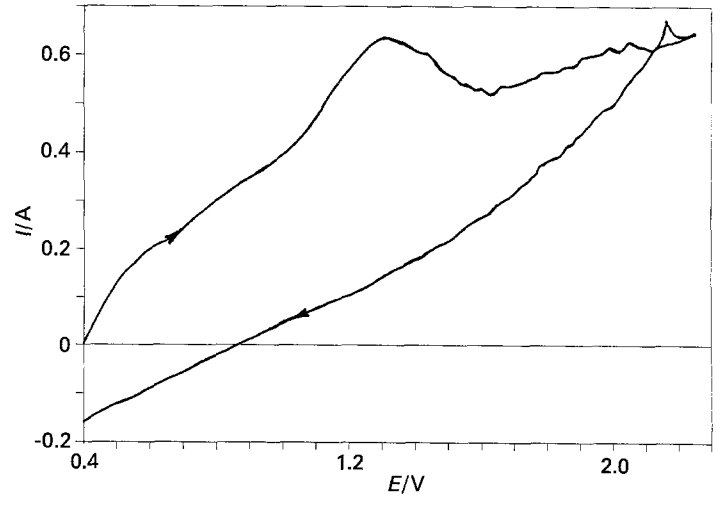

Fig. 9. Cyclic voltammogram for a stainless steel working electrode (10 g Al_2O_3 added in the cryolite melt, sweep rate $0.3\,V\,s^{-1}$).

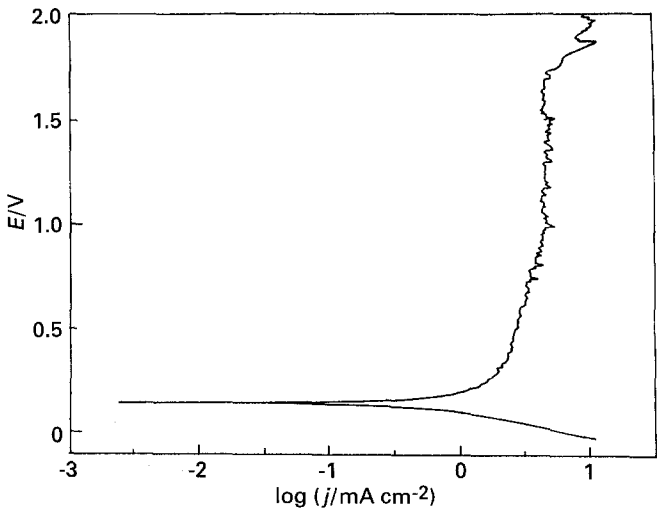

Fig. 10. Anodic Tafel polarization curve for a glassy carbon in a melt containing 30 g Al_2O_3 per 650 g cryolite.

experiments were restricted to sweep rates less than $1\,V\,s^{-1}$. On the increasing potential side of the cyclic voltammogram, can be seen an anodic peak at about 1.3 V (Fig. 9). However, in the negative-going sweep in the voltammograms, no cathodic currents arise; this behaviour indicates, of course, a severe irreversibility of the process involved. It was found that an increase in square-root of sweep rate leads to some increase in peak current. The potential of the anodic peak did not, however, change with increase of sweep rate in the case of lower alumina concentrations. For the melts with higher alumina concentrations, the potential of the anodic peak became changed from 1.18 to 1.55 V with increase of sweep rate from 0.1 to $0.5\,V\,s^{-1}$. However, the dependence of peak current on alumina concentration again did not follow any significant systematic trend suitable for an analytical application.

Based on chronoamperometric measurements at the stainless steel electrode, the dependencies of I^{-1} vs $t^{1/2}$ do not follow the linear relationship expected for diffusion control, as also found for the other anodes investigated.

The peak at about 1.3 V could be related to the discharge of oxygen-containing species leading to formation of various oxides, as films, which become dissolved in the cryolite at elevated temperatures. As in the case of the other metals, SEM photography showed that the stainless steel anode becomes consumed in the cryolite medium.

3.5. *Glassy carbon electrode*

The failure, even of WC, as an anode probe material for electroanalytical determination of Al_2O_3 in cryolite melts led us to examine glassy carbon as a possible nonconsumable material. In this case, the experiments were more successful, as described below.

First, the open-circuit potential in these experiments was quite consistent. It had, most commonly, stable values at about 0.4 V vs Al. Figure 10 shows the anodic Tafel plot for this material and it exhibits a clear approach to a *limiting current* thus corresponding to diffusion control; agitation of the melt increases this current appreciably but in an irregular way. Also, current irregularities arise due to unavoidable formation and detachment of CO or CO_2 bubbles from the carbon surface, confirming the role of diffusion control.

In Fig. 11 is shown a cyclic voltammogram obtained at the glassy carbon electrode over the potential range 0.4 to 2.25 V vs Al. This voltammogram displays a significant anodic peak at a potential of about 1.8 V which increases from 1.6 to 2.0 V (depending on the Al_2O_3 content in the bath) with increase of sweep rate from 10 to $80\,V\,s^{-1}$. This peak

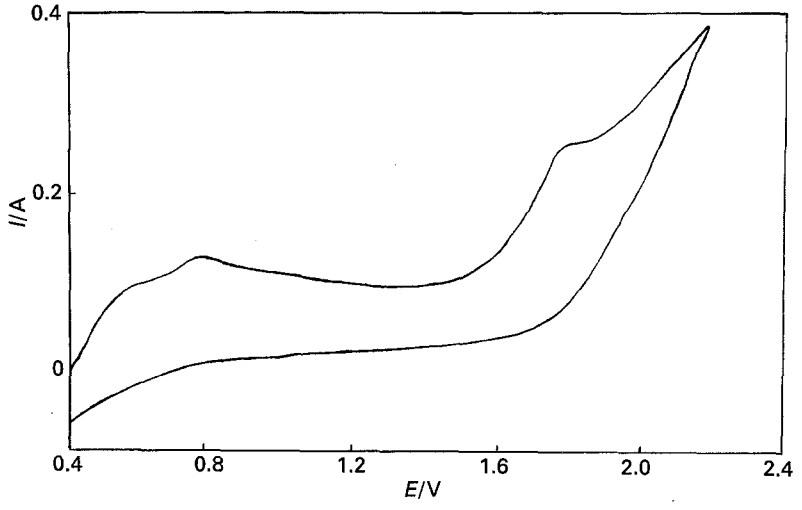

Fig. 11. Cyclic voltammogram for anodic oxidation process at glassy carbon electrode (10 g Al_2O_3, sweep rate $80\,V\,s^{-1}$).

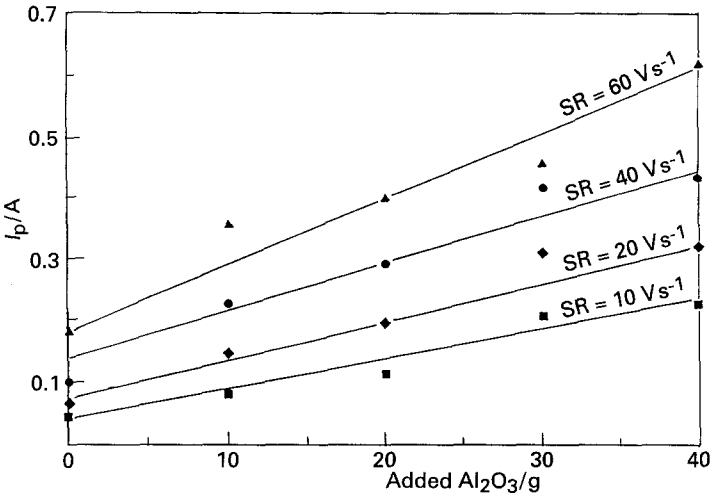

Fig. 12. Dependence of peak current in cyclic voltammetry at glassy carbon on Al_2O_3 content in the melt for different sweep rates (working electrode: glassy carbon, sweep potential range from 0.4 to 2.25 V vs Al reference electrode) [18].

was attributed to the discharge of oxygen-containing species [18]. Furthermore, the peak currents depend quite linearly on square-root of sweep rate, the characteristic feature of diffusion control. This is also consistent with the shape of the Tafel plot in Fig. 10. Finally, the dependence of peak current on Al_2O_3 content in the melt was found to follow a *linear relationship* as presented in Fig. 12. The conclusions reached from the combination of cyclic voltammetry and Tafel polarization experiments [18] were confirmed by chronoamperometry [19] which showed that a plot of the current function ($It^{1/2}$) evaluated from chronoamperometric I–t curves vs Al_2O_3 content in the melt, follows a satisfactorily linear relationship providing also a basis for application of this method for analytical purposes.

4. Conclusions

Comparative experiments at a series of anode materials, including glassy carbon, show that results obtained at the latter material used as an indicator electrode for Al_2O_3 determination are, by far, the most satisfactory for establishing a meaningful electroanalytical response current, i.e. one linear in the anolyte concentration. On the other hand, metals such as W, WC, Ni and SS-316 in cryolite/alumina melts at 1010° C are unresistant as anodes for the Hall–Héroult process or as anodes for analytical probes. Consequently, the results obtained by electroanalytical techniques are not reproducible nor are they systematically related to Al_2O_3 concentration as required for *in situ* analytical application. Thus, the results obtained have demonstrated that the metals, or WC, investigated cannot be used as anodes for determination of alumina in alumina cryolite melts nor, implicitly, as materials for the main cell anodes in the electrolytic smelter. However, for a detailed explanation or understanding of the processes involved at anode materials investigated (W, WC, Ni and SS-316) in cryolite melt at elevated temperatures, more experimental studies are needed.

Acknowledgements

Grateful acknowledgement is made to Alcan International Ltd., Arvida Research Laboratory, for support of this work. We also acknowledge matching fund support from the Ontario University Research Incentive Fund.

References

[1] A. I. Belyaev and Ya. E. Studentsov, *Legkie Metall* **6**(3), (1937) 17.
[2] A. I. Belyaev, *ibid.* **7**(1), (1938) 7.
[3] B. Marincek, *Schweiz. Arch. Agnew. Wiss. Tech.* **33** (1967) 395.
[4] H. Alder, *US Patent 3 930 967* (1976).
[5] *Idem, US Patent 3 974 046* (1976).
[6] *Idem, US Patent 3 960 678* (1976).
[7] V. De Nora, P. M. Spazinate and A. Nidola, *US Patent 4 098 669* (1978).
[8] C. F. Windisch Jr. and S. C. Marschman, 'Light Metals', Proceedings of the technical sessions sponsored by the TMS Light Metal Committee at 116th Annual Meeting, Denver, Colorado, 24–26 Feb. (1987) p. 351.
[9] K. Billehaug and H. A. Øye, *Aluminium* **57** (1981) 146.
[10] M. Rollin, *Bul. Soc. Fr. Electr. Ser.* 8, T6, **70** (1965) 689.
[11] A. S. Galkov, *USSR Patent 454 309* (1974).
[12] H. T. Shiver, J. L. Dewey and W. E. Campbell, *French Patent 1 457 746*.
[13] M. L. Kronenberg, *J. Electrochem. Soc.* **116** (1969) 1160.
[14] V. V. Stender and V. V. Trofimenko, *Khim. Tekhnol.* **12** (1969) 41.
[15] J. Thonstad, *Electrochim. Acta.* **13** (1968) 449.
[16] K. Grjotheim, C. Krohn, M. Malinovský, K. Matiašovský and J. Thonstad, 'Aluminium electrolysis – Fundamentals of the Hall–Héroult Process', 2nd edn, Aluminium-Verlag, Düsseldorf (1982).
[17] E. W. Dewing and E. T. Van der Kouwe, *J. Electrochem. Soc.* **124** (1977) 58.
[18] S. S. Djokić, B. E. Conway and T. F. Belliveau, *J. Appl. Electrochem.*, **24** (1994) 827.
[19] *Idem, J. Electrochem. Soc.*, **141** (1994) 2106.